Enhancing Mechanical Properties of a Lightweight TiAlCrNbVZr Medium-Entropy Alloy: Fine-Tuning Alloy Composition and Thermomechanical Treatment

Po-Sung Chen[1], Ting-Wei Sung[2], Pei-Hua Tsai[1], Yu-Chin Liao[2], Jason Shian-Ching Jang[1,2,*], Hsin-Jay Wu[3], Shou-Yi Chang[4], Chih-Yen Chen[5] and I-Yu Tsao[1]

[1]*Institute of Materials Science and Engineering, National Central University, Zhongli 320, Taiwan*

[2]*Department of Mechanical Engineering, National Central University, Zhongli 320, Taiwan*

[3]*Department of Materials Science and Engineering, National Yang Ming Chiao Tung University, Hsinchu 300, Taiwan*

[4]*Department of Materials Science and Engineering, National Tsing Hua University, Hsinchu 300, Taiwan*

[5]*Department of Electrophysics, National Yang Ming Chiao Tung University, Hsinchu 300, Taiwan*

Abstract: The quest to reduce fuel consumption and environmental pollution in the transportation sector has heightened the demand for developing lightweight alloys with enhanced mechanical properties. Accordingly, this study focused on optimizing the mechanical properties of a lightweight $Ti_{65}(AlCrNbV)_{28}Zr_7$ medium entropy alloy (MEA) by strategically adjusting its Al, Cr, Nb, and V elemental contents. Hardness testing indicated a strengthening ability hierarchy of Cr > Al > V > Nb. Furthermore, tensile tests revealed that although a high Cr content significantly enhances strength, it also reduces the ductility of an MEA. Drawing on mechanical insights gained from a previously studied $Ti_{60}Al_{10}Cr_{10}Nb_{10}V_{10}$ MEA and the present findings, a novel $Ti_{60}Al_{10}Cr_4Nb_{10}V_9Zr_7$ (Ti60Zr7) MEA was developed. This new alloy retains a single body-centered cubic structure and demonstrated exceptional mechanical performance in tensile testing, with a yield strength of 1066 MPa and 22% ductility. The Ti60Zr7 MEA underwent a series of thermomechanical treatments, including 50% hot rolling, 80% cold rolling, and rapid annealing up to 800 °C at a rate of 25 °C/s. After thermal processing, the Ti60Zr7 MEA not only preserved its single body-centered cubic structure but also achieved a remarkable combination of yield strength (>1200 MPa) and ductility (measured as >15% elongation). These advancements underscore the alloy's considerable potential for application in sports equipment and transportation vehicles.

Keywords: Medium-entropy alloy, Light-weight, Non-equiatomic, Composition adjustment, Thermo-mechanical treatment, Mechanical property optimization.

INTRODUCTION

In recent decades, the sports goods and transportation industries have increasingly demanded lightweight materials such as Al, Ti, and Mg alloys [1]. Ti alloys—known for their high strength, toughness, and excellent corrosion resistance—are widely used in structural material and bioimplants. Traditional alloy design, however, encounters a limitation: An alloy with a high proportion of solute elements tends to precipitate intermetallic compounds during deformation, leading to brittleness [2]. This consequence limits the properties of the traditional alloy and restrict the range of the alloy design [3, 4]. Therefore, innovative alloy designs that transcend traditional concepts are essential.

Related studies have focused on Ti-rich high entropy alloys (HEAs) and medium entropy alloys (MEAs) [5, 6]. These novel alloys maintain the individual features of their component elements and also expand the range of microalloying beyond the traditional alloy design parameters [7-9]. HEAs and MEAs are characterized by structures primarily composed of simple solid solutions and thus eschew the formation of complex phases or intermetallic compounds [10, 11]. In addition, they exhibit enhanced thermal stability and mechanical properties compared with commercial alloys, highlighting their industrial applicability [12, 13]. Moreover, the distinctive so-called cocktail effect of HEAs and MEAs both simplifies and enhances alloy modification [14-16]. The development of Ti-rich HEAs and MEAs is advancing; some variants even demonstrate superior properties to traditional materials, suggesting their potential to replace commercial materials in future applications [17, 18].

To further enhance the mechanical properties of an alloy, thermomechanical treatment (TMT) is essential to modify the alloy's structure and augment its strength and ductility [19-22]. Hot working techniques can refine the grain size of the alloy and eliminate defects from casting, whereas cold working accumulates strain energy, which provides the necessary energy for recrystallization during annealing. Additionally, rapid thermal processing is conducted [23-24]; this process, which involves high-temperature but brief annealing, yields significantly smaller recrystallized grains

*Address correspondence to this article at the Institute of Materials Science and Engineering, National Central University, Zhongli 320, Taiwan;
E-mail: jscjang@ncu.edu.tw

E-ISSN: 2410-4701/24 © 2024 Zeal Press

compared with conventional annealing and thus enhances the overall mechanical properties of the alloy through grain boundary strengthening.

The present study extended previous research regarding a $Ti_{65}(AlCrNbV)_{28}Zr_7$ MEA [18] by adjusting the combination of Al, Cr, Nb, and V elements to determine the strengthening ability of each element in this MEA. The aim was to develop a modified alloy composition for a novel Ti-rich MEA with optimum as-cast mechanical properties. The novel Ti-rich MEAs were subjected to a hot rolling process with a 50% reduction and a cold rolling process with a 70% reduction (HR50CR70) followed by rapid annealing to further enhance the mechanical properties. The primary objective of this study was to develop a lightweight Ti-rich MEA (approximately 5 g/cm^3) with a combination of high yield strength (1200 MPa) and high ductility (15 %).

EXPERIMENTAL PROCEDURE

Materials

As mentioned, this study employed a previously studied $Ti_{65}(AlCrNbV)_{28}Zr_7$ MEA, known for its impressive mechanical properties, as its base alloy. The objective was to fine-tune the elemental contents of Al, Cr, Nb, and V and evaluate these elements' individual strengthening effects on the Ti-rich MEA. Six variations of Ti-rich MEAs were designed: $Ti_{65}Al_xCr_yNb_zV_wZr_7$ (x, y, z, w: 4, 4, 10, 10), including $Ti_{65}Al_{10}Cr_{10}Nb_4V_4Zr_7$ (Al10Cr10), $Ti_{65}Al_{10}Cr_4Nb_{10}V_4Zr_7$ (Al10Nb10), $Ti_{65}Al_{10}Cr_4Nb_4V_{10}Zr_7$ (Al10V10), $Ti_{65}Al_4Cr_{10}Nb_{10}V_4Zr_7$ (Cr10Nb10), $Ti_{65}Al_4Cr_{10}Nb_4V_{10}Zr_7$ (Cr10V10), and $Ti_{65}Al_4Cr_4Nb_{10}V_{10}Zr_7$ (Nb10V10). Master alloys were fabricated through arc-melting using high-purity raw materials (Al [99.99%], Ti [99.99%], Nb [99.99%], Cr [99.99%], V [99.9%], and Zr [99.99%]) in an argon atmosphere with Ti-getter to prevent oxidation. Each master alloy was melted initially and then remelted three times to ensure compositional homogeneity. Subsequently, the alloys were drop-cast into ingots measuring 50 mm (length) × 20 mm (width) × 10 mm (thickness).

Thermomechanical Treatment

Initially, the aforementioned ingots underwent homogenization at 1000 °C for 2 h in a high-vacuum atmosphere (10^{-6} mbar) followed by rapid water quenching to prevent segregation. Subsequently, the homogenized ingots were hot-rolled at 1000 °C with a 50% thickness reduction; this process was followed by cold rolling at room temperature with a 70% thickness reduction (HR50CR70). The deformed specimens then underwent rapid annealing (heating rate: 25 °C/s) at multiple temperatures in a high-vacuum atmosphere (10^{-6} mbar) to modify the microstructure and improve the mechanical properties of the alloy.

Microstructure Characterization

The density of each MEA was measured using Archimedes' principle. In addition, X-ray diffraction (XRD; D2, Bruker, Billerica, MA, USA) was performed with Cu-Kα radiation. The morphology was observed using optical microscopy (OM; BX51M, Olympus, Tokyo, Japan) and electron backscatter diffraction (EBSD; HKL Channel 5, Oxford Instruments, Hobro, Denmark). For XRD analysis, the samples were ground using silicon carbide sandpaper from #80 to #2000 grit. For OM, the samples were polished with 1, 0.3, and 0.05 μm Al_2O_3 suspension liquid. Finally, for EBSD, the samples underwent electropolishing.

Mechanical Testing

The hardness of each MEA was measured using a Vickers hardness tester (HV-115; Mitutoyo, Kawasaki, Japan) with a 5-kg load for 10 s. The tensile properties were analyzed using a universal testing machine (HT9102; Hung Ta, Taichung, Taiwan) under quasistatic loading at a strain rate of 1×10^{-4} s^{-1}. For hardness testing, the samples were ground using silicon carbide sandpaper from #80 to #2000 grit. Tensile testing samples with a gauge dimension of 5 mm (length) × 2 mm (width) × 1.5 mm (thickness) were then fabricated.

RESULTS AND DISCUSSION

This study was divided into two primary parts. The first part involved fine-tuning the composition of the previously researched $Ti_{65}(AlCrNbV)_{28}Zr_7$ MEA to identify the strengthening effects of Al, Cr, Nb, and V on the MEA. The second part focused on developing a novel Ti-rich MEA composition and applying TMT to improve this alloy's mechanical performance.

Identifying the Strengthening Abilities of Al, Cr, Nb, and V With Respect to the MEAs

Despite variations in the proportions of minor elements across the Ti-rich MEAs, the MEAs' configuration entropy uniformly remained at 9.85 because of the 4-4-10-10 configuration of these elements. This entropy value categorized them as MEAs, as illustrated in Table **1**. The atomic size differences (δ) among these alloys were calculated using Equation (1) [25]:

$$\delta = 100\sqrt{\sum_{i=1}^{n} c_i(1 - r_i/\bar{r})^2} \quad (1)$$

Table 1: The Parameters of the as-Cast $Ti_{65}Al_xCr_yNb_zV_wZr_7$ (x, y, z, w: 4, 4, 10, 10) MEAs

Composition	ΔS (kJ. mol^{-1})	δ (%)	Lattice Constant (Å)
Al10Cr10	9.85	4.99	3.230
Al10Nb10	9.85	3.99	3.274
Al10V10	9.85	4.47	3.251
Cr10Nb10	9.85	4.98	3.254
Cr10V10	9.85	5.33	3.219
Nb10V10	9.85	4.45	3.263

where $\bar{r} = \sum_{i=1}^{n} c_i r_i$ and where c_i and r_i represent the atomic fraction and atomic radius of the *i*th element, respectively. The atomic size difference across all the MEAs was approximately 5%, which was conducive to the formation of a single solid solution structure, as indicated in Table **1**.

The densities of the as-prepared MEAs were measured using Archimedes' principle and were found to be similar to their corresponding theoretical densities calculated using the mixing rule [18], as presented in Table **2**. The densities of these Ti-rich MEAs were approximately 5 g/cm^3; this result aligned with the present study's goal of creating lightweight materials. However, an increase in the proportion of heavier elements such as Cr and Nb resulted in a corresponding slight increase in the overall density of the Ti-rich MEAs.

The XRD results revealed that all the series MEAs exhibited the peaks characteristic of a body-centered cubic (BCC) structure, as illustrated in Figure **1**. The approximately 5% atomic size difference supported the formation of a solid solution structure. Furthermore, notable shifts in the diffraction peaks were observed. An increase in the proportion of elements with a larger atomic radius, particularly Al and Nb, caused a leftward shift of the diffraction peaks, indicating an increase in the overall lattice constant of the MEAs.

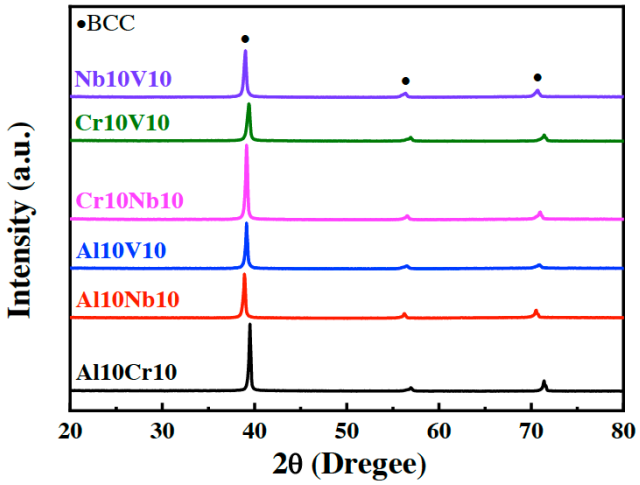

Figure 1: The XRD patterns of the as-cast $Ti_{65}Al_xCr_yNb_zV_wZr_7$ (x, y, z, w: 4, 4, 10, 10) MEAs.

Regarding mechanical testing, the results of hardness and tensile tests are summarized in Table **3**. Alloys containing higher concentrations of Al and Cr more clearly exhibited enhanced hardness compared with other studied MEAs, with the Al10Cr10 alloy exhibiting the highest hardness. However, the Al10Cr10 alloy also exhibited excessive brittleness, resulting in negligible plasticity during tensile testing. Conversely, the alloys with high proportions of Nb and V exhibited lower hardness but higher ductility. Overall, based on the obtained hardness and tensile testing data, the strengthening abilities of the minor elements were ranked as Cr > Al > V > Nb, as presented in Figure **2**.

Table 2: The Density of the as-Cast $Ti_{65}Al_xCr_yNb_zV_wZr_7$ (x, y, z, w: 4, 4, 10, 10) MEAs

Composition	Theoretical Density (g/cm^3)	Measured Density (g/cm^3)	Error (%)
Al10Cr10	4.98	4.91	1.40
Al10Nb10	5.06	5.14	1.58
Al10V10	4.92	5.04	2.43
Cr10Nb10	5.34	5.28	1.12
Cr10V10	5.19	5.17	0.38
Nb10V10	5.27	5.28	0.19

Table 3: The Hardness and Tensile Mechanical Properties of the as-Cast $Ti_{65}Al_xCr_yNb_zV_wZr_7$ (x, y, z, w: 4, 4, 10, 10) MEAs

Composition	Hardness (HV)	Yield Strength (MPa)	Ultimate Strength (MPa)	Ductility (%)
Al10Cr10	371 ± 8	Rupture		
Al10Nb10	318 ± 5	959 ± 17	1068 ± 25	23 ± 1
Al10V10	333 ± 7	1035 ± 4	1078 ± 15	12 ± 3
Cr10Nb10	328 ± 7	987 ± 3	1082 ± 1	9 ± 1
Cr10V10	339 ± 2	1030 ± 14	1079 ± 18	4 ± 1
Nb10V10	292 ± 5	850 ± 16	1008 ± 29	19 ± 1

Remarks: The Al10Cr10 broke before passing the yielding point.

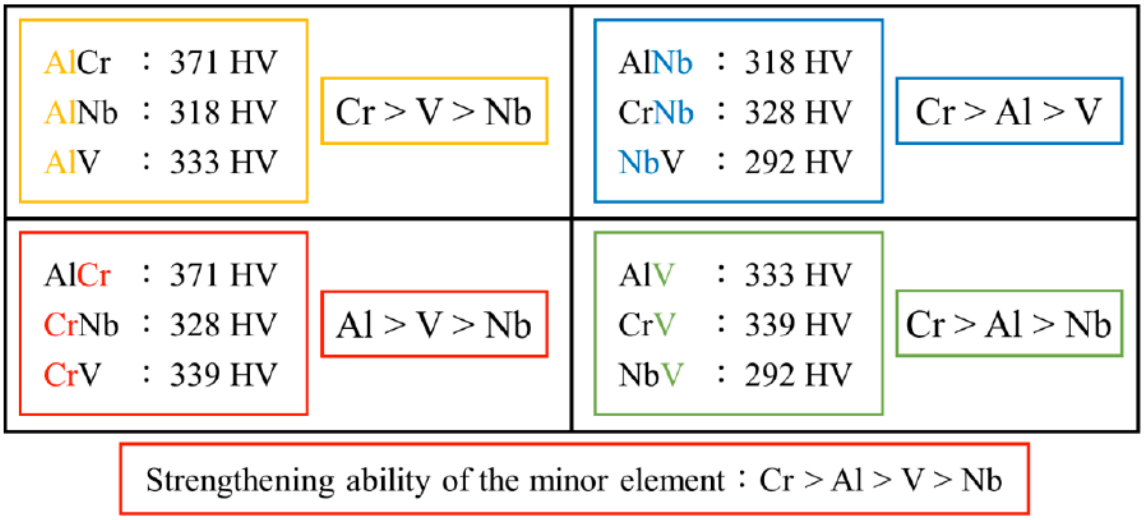

Figure 2: The hardness comparison of the as-cast $Ti_{65}Al_xCr_yNb_zV_wZr_7$ (x, y, z, w: 4, 4, 10, 10) MEAs.

Exploration of Novel Ti-rich MEAs

Drawing from insights in our previous study [17], observations in the present study indicated that a higher concentration of Ti in Ti-rich MEAs typically leads to a reduction in their strength. However, adding V content not only enhances the ductility of an MEA but also maintains its strength level [18]. The present study found that a high Cr content significantly improves strength but drastically reduces the ductility of an MEA. Accordingly, on the basis of these insights, a novel Ti-rich MEA, namely $Ti_{60}Al_{10}Cr_4Nb_{10}V_9Zr_7$ (Ti60Zr7), was developed. The density of the Ti60Zr7 MEA is approximately 5.16 g/cm^3, which qualifies it as a lightweight material. Moreover, the Ti60Zr7 MEA maintains a simple BCC solid solution structure, as presented in Figure **3**.

To compare the mechanical properties of as-cast Ti-rich MEAs from the present study and relevant studies, results related to the hardness and tensile properties of Ti60Zr7 and earlier Ti-rich MEAs are listed in Table **4**. The as-cast Ti60Zr7 MEA exhibits an excellent combination of yield strength and ductility, achieving a yield strength of 1066 MPa with 23% ductility. This performance surpasses those of MEAs in relevant studies [17, 18, 26], as illustrated in Figure **4**.

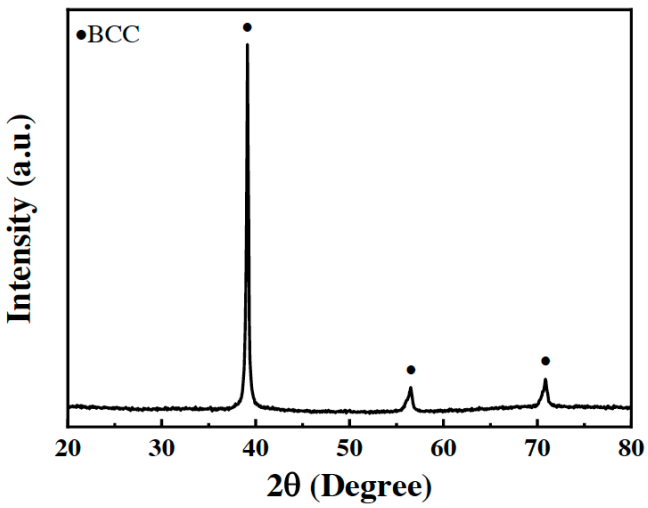

Figure 3: The XRD patterns of the as-cast Ti60Zr7 MEA.

Table 4: The Hardness and Tensile Mechanical Properties of the as-Cast Ti60Zr7 MEAs and Previous Studies

Composition	Hardness (HV)	Yield Strength (MPa)	Ultimate Strength (MPa)	Ductility (%)
Ti65	323 ± 5	954 ± 19	1136 ± 26	20 ± 2
Ti60Al8	321 ± 2	920 ± 8	1146 ± 15	29 ± 1
Ti65Ni3	355 ± 7	1065 ± 3	1230 ± 40	18 ± 2
Ti65Zr7	331 ± 4	1015 ± 26	1170 ± 14	22 ± 2
Ti60Zr7	350 ± 7	1066 ± 3	1186 ± 33	23 ± 2

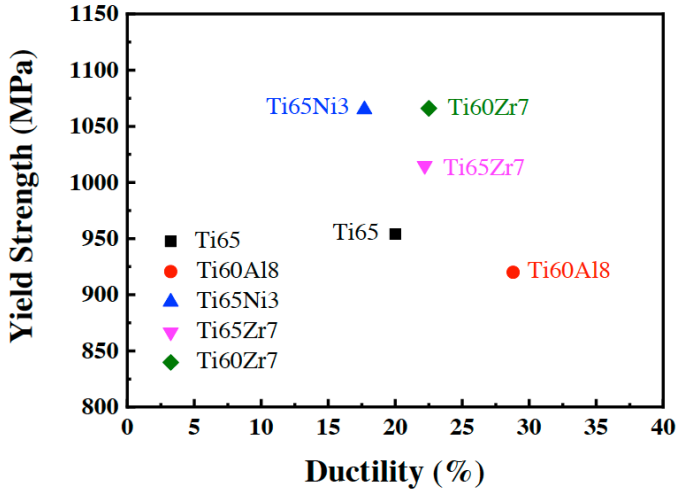

Figure 4: Comparison of yield strength and ductility for the as-cast Ti60Zr7 MEA to the previous studies.

To further enhance the mechanical properties of the Ti60Zr7 MEA, TMT and rapid annealing were conducted in the present study. The alloy was homogenized at 1000 °C for 2 h and was hot-rolled to 50% reduction to counteract compositional inhomogeneity due to casting. Then, the alloy was cold-rolled by 80% (HR50CR80) to accumulate strain energy for subsequent recrystallization. The final step involved rapid annealing at temperatures of 650, 700, 750, and 800 °C with a heating rate of 25 °C/s.

Figure **5** displays the XRD results for the as-rolled and annealed samples. Notably, all the samples retained a single BCC structure, evident in the as-rolled and annealed states. This outcome indicates that the Ti60Zr7 MEA exhibits high solid solution phase stability. During the annealing process, observations revealed the onset of sample recrystallization at 750 °C accompanied by an escalation in the degree of recrystallization correlating to rising annealing temperatures, as illustrated by the OM and EBSD images presented in Figure **6** and Figure **7**.

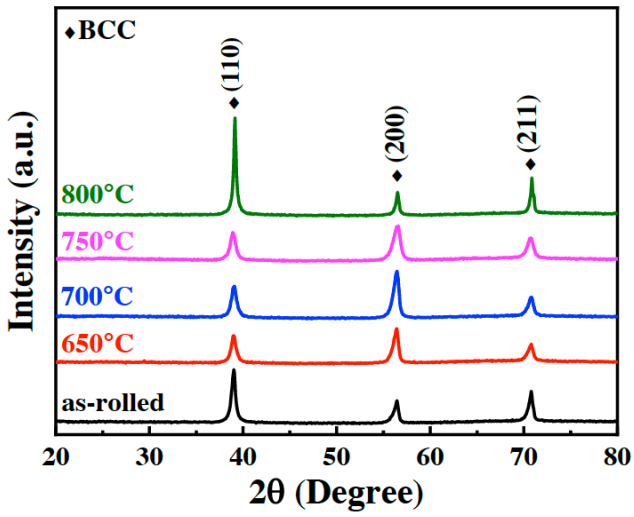

Figure 5: The XRD patterns of HR50CR80 Ti60Zr7 MEA with different annealing temperatures.

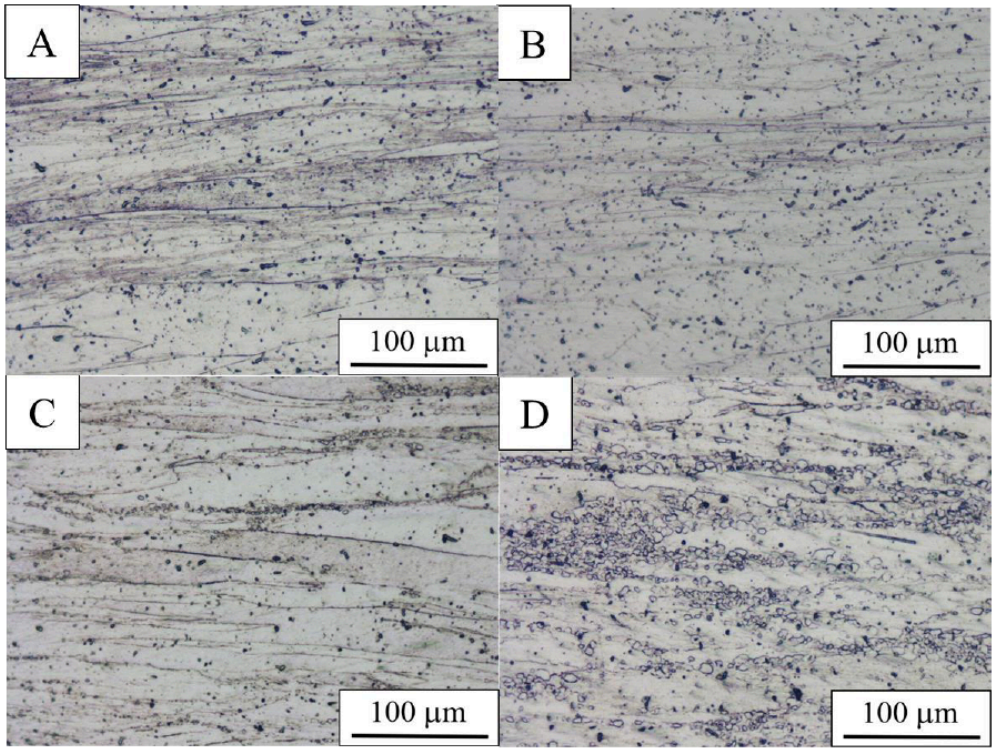

Figure 6: The OM images of HR50CR80 Ti60Zr7 MEA with different annealing temperatures. (**A**) 650°C; (**B**) 700°C; (**C**) 750°C; (**D**) 800°C.

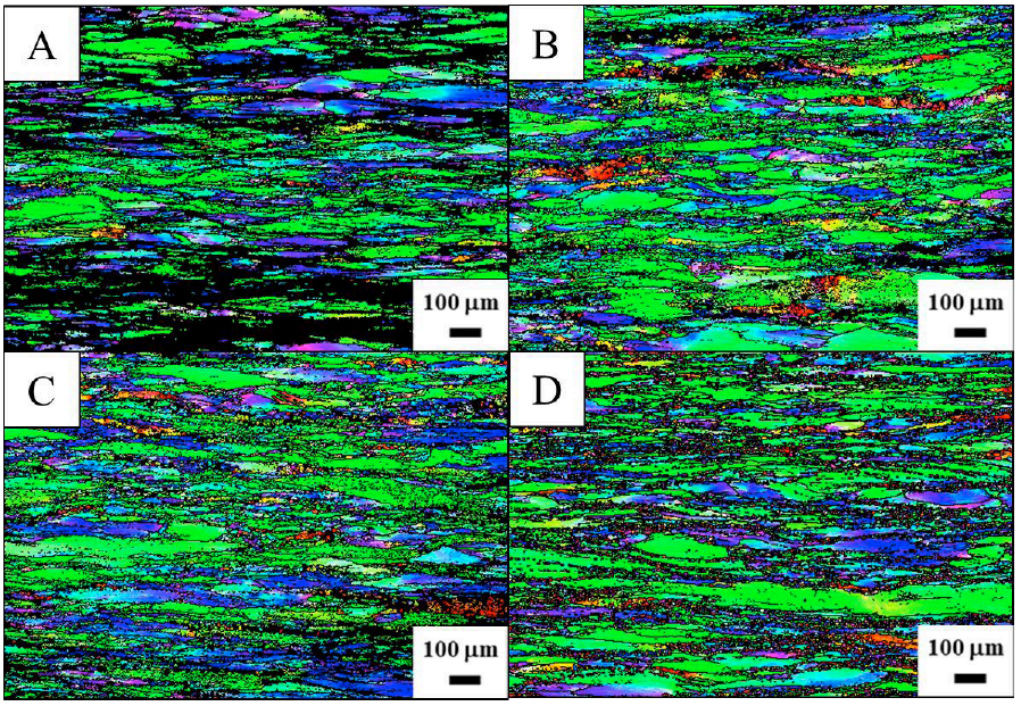

Figure 7: The EBSD images of HR50CR80 Ti60Zr7 MEA with different annealing temperatures. (**A**) 650°C; (**B**) 700°C; (**C**) 750°C; (**D**) 800°C.

After undergoing 80% cold rolling, the as-rolled sample exhibited its highest strength, namely 1543 MPa, but also showed reduced ductility by 5%. As the annealing temperature increased, the yield strength evidently decreased and the ductility significantly increased, as illustrated in Figure **8** and Table **5**, respectively. The optimal balance of yield strength and ductility was achieved in the sample annealed at 700 °C. In summary, the Ti60Zr7 MEA, subjected to HR50CR80 processing and annealed at 700 °C with a rapid heating rate of 25 K/s, demonstrated excellent synergy of mechanical properties. The yield strength exceeded 1200MPa, and ductility of 15% was demonstrated.

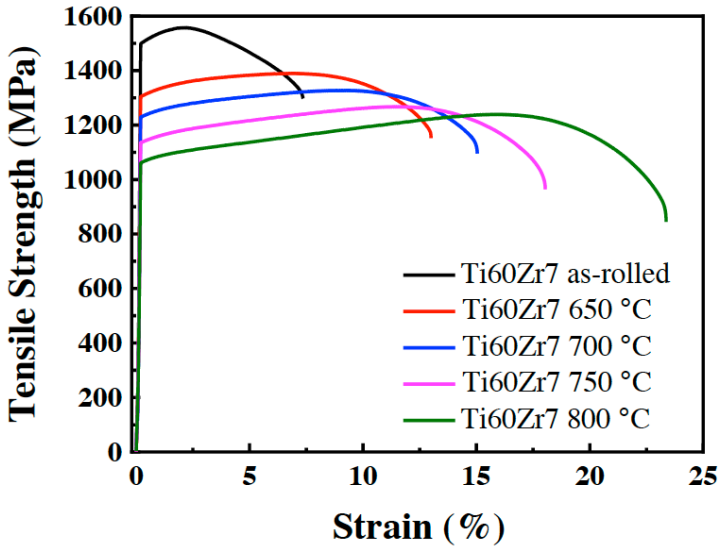

Figure 8: The mechanical tensile stress–strain curves of HR80CR80 Ti60Zr7 MEA with different annealing temperature.

Table 5: Tensile Mechanical Properties of Ti60Zr7 MEAs with Different Annealing Temperature

Composition	Yield Strength (MPa)	Ultimate Strength (MPa)	Ductility (%)
as-rolled	1543 ± 64	1598 ± 57	5 ± 3
650°C	1330 ± 37	1416 ± 36	11 ± 2
700°C	1212 ± 23	1313 ± 15	15 ± 1
750°C	1123 ± 18	1254 ± 10	17 ± 1
800°C	1073 ± 16	1233 ± 10	22 ± 2

CONCLUSION

In this study, a series of alloy compositions of Ti-rich MEAs, specifically $Ti_{65}Al_xCr_yNb_zV_wZr_7$ (x, y, z, w: 4, 4, 10, 10), was investigated to ascertain the strengthening capabilities of minor elements. Subsequently, this study, using insights gained from previous studies, developed a novel Ti60Zr7 MEA. The key findings and conclusions are summarized as follows:

1. The $Ti_{65}Al_xCr_yNb_zV_wZr_7$ and Ti60Zr7 MEAs exhibited a single BCC structure. However, the addition of Cr and Nb increased the alloy's density, which ranged from 4.98 to 5.34 g/cm^3.

2. An analysis of hardness and tensile testing data for the nonequiatomic $Ti_{65}Al_xCr_yNb_zV_wZr_7$ MEAs revealed the following hierarchy in the strengthening ability of elements: Cr > Al > V > Nb. Notably, a high Cr content significantly improved strength but markedly reduced the ductility of the MEAs.

3. This study leveraged knowledge gained from previous studies and the current level of understanding of the strengthening effects of minor elements to develop a novel Ti-rich MEA, namely $Ti_{60}Al_{10}Cr_4Nb_{10}V_9Zr_7$ (Ti60Zr7). The density of the Ti60Zr7 MEA was approximately 5.16 g/cm^3, which confirmed its status as a lightweight material.

4. The as-cast Ti60Zr7 MEA exhibited an excellent combination of yield strength and ductility. Specifically, it achieved a yield strength of 1066 MPa with 23% ductility and thus surpassed the performances of previously developed Ti-rich MEAs documented in related studies.

5. Overall, the Ti60Zr7 MEA, processed using HR50CR80 and annealed at 700 °C with a rapid heating rate of 25 K/s, demonstrated an excellent combination of mechanical properties. It achieved a yield strength of over 1200 MPa and ductility of 15%.

AUTHOR CONTRIBUTIONS

Conceptualization, J.S.-C.J. and P.-S.C.; formal analysis, P.-S.C., T.-W.S., and I.-Y.T.; resources, Y.-C.L. and T.-W.S.; data curation, P.-S.C. and T.-W.S.; writing—original draft preparation, P.-S.C.; writing—review and editing, J.S.-C.J.; supervision, P.-H.T., J.S.-C.J., H.-J.W., S.-Y.C., and C.-Y.C.. All

authors have read and agreed to the published version of the manuscript.

FUNDING

The financial support of the Ministry of Science and Technology of Taiwan, Republic of China (MOST 110-2221-E-008-090) and the National Science and Technology Council, Taiwan (NSTC 111-2224-E-008-001) is gratefully acknowledged.

INSTITUTIONAL REVIEW BOARD STATEMENT

Not applicable.

INFORMED CONSENT STATEMENT

Not applicable.

DATA AVAILABILITY STATEMENT

Data are contained within the article.

ACKNOWLEDGMENTS

The authors express gratitude for the support provided by the Ministry of Science and Technology of Taiwan, Republic of China (MOST 110-2221-E-008-090) and the National Science and Technology Council, Taiwan (NSTC 111-2224-E-008-001), and the analytical assistance offered by the Precision Instrument Center of National Central University. Additionally, the authors acknowledge the Department of Materials Science and Engineering, I-Shou University, for providing access to their experimental equipment.

CONFLICTS OF INTEREST

The authors declare no conflict of interest.

REFERENCES

[1] Aluminum-Lithium Alloys Fight Back. https://aluminiuminsider.com/aluminium-lithium-alloys-fight-back/

[2] Springer, H., Baron, C., Szczepaniak, A., Uhlenwinkel, V., & Raabe, D. (2017). Stiff, light, strong and ductile: nano-structured High Modulus Steel. Scientific Reports, 7(1). https://doi.org/10.1038/s41598-017-02861-3

[3] ASM International. Handbook Committee, “Properties and Selection: Irons, Steels, and High-Performance Alloys”; ASM International: Materials Park, OH, USA, 1990; Volume 1.

[4] ASM International. Handbook Committee, “Properties and Selection: Nonferrous Alloys and Special-Purpose Materials”; ASM International: Materials Park, OH, USA, 1990; Volume 2.

[5] Huang, K.H.; Yeh, J.W. A Study On Multicomponent Alloy Systems Containing Equal-Mole Elements; Department of Materials Science and Engineering, Hsinchu: National Tsing Hua University: Beijing, China, 1996.

[6] Yeh, J.W.; Chen, S.K.; Lin, S.J.; Gan, J.Y.; Chin, T.S.; Shun, T.T.; Tsau, C.H.; Chang, S.Y. Nanostructure High-Entropy Alloys with Multiple Principle Elements: Novel Alloy Design Concepts and Outcomes. Adv. Eng. Mater. 2004, 6, 299-303. https://doi.org/10.1002/adem.200300567

[7] Yao, M.; Pradeep, K.; Tasan, C.; Raabe, D. A novel, single phase, non-equiatomic FeMnNiCoCr high entropy alloy with exceptional phase stability and tensile ductility. Scr. Mater. 2014, 72–73, 5-8. https://doi.org/10.1016/j.scriptamat.2013.09.030

[8] Youssef, K.; Zaddach, A.J.; Niu, C.; Irving, D.L.; Koch, C.C. A Novel Low-Density, High-Hardness, High-entropy Alloy with Close-packed Single-phase Nanocrystalline Structures. Mater. Res. Lett. 2014, 3, 95-99. https://doi.org/10.1080/21663831.2014.985855

[9] Stepanov, N.; Shaysultanov, D.; Chernichenko, R.; Tikhonovsky, M.; Zherebtsov, S. Effect of Al on structure and mechanical properties of Fe-Mn-Cr-Ni-Al non-equiatomic high entropy alloys with high Fe content. J. Alloys Compd. 2019, 770, 194-203. https://doi.org/10.1016/j.jallcom.2018.08.093

[10] Li, R.; Gao, J.; Fan, K. Study to Microstructure and Mechanical Properties of Mg Containing High Entropy Alloys. Mater. Sci. Forum 2010, 650, 265-271. https://doi.org/10.4028/www.scientific.net/MSF.650.265

[11] Du, X.;Wang, R.; Chen, C.;Wu, B.; Huang, J. Preparation of a Light-Weight MgCaAlLiCu High-Entropy Alloy. Key Eng. Mater. 2017, 727, 132-135. https://doi.org/10.4028/www.scientific.net/KEM.727.132

[12] Yeh, J.W. Recent progress in high-entropy alloys. Ann. Chim. Sci. Mat. 2006, 31, 633-648. https://doi.org/10.3166/acsm.31.633-648

[13] Yeh J. W.; Chang S. Y.; Honga Y. D.; Chenc S. K.; Lin, S. J. Anomalous decrease in X-ray diffraction intensities of Cu–Ni–Al–Co–Cr–Fe–Si alloy systems with multi-principal elements. Materials Chemistry and Physics, 2007, 103, 41-46. https://doi.org/10.1016/j.matchemphys.2007.01.003

[14] Li, Z.; Pradeep, K. G.; Deng, Y.; Raabe, D.; Tasan, C. C. Metastable high-entropy dual-phase alloys overcome the strength-ductility trade-off. Nature. 2016, 534(7606), 227-230. https://doi.org/10.1038/nature17981

[15] Li, Z.; Raabe, D. Strong and Ductile Non-equiatomic High-Entropy Alloys: Design, Processing. Microstructure, and Mechanical Properties. JOM. 2017, 69, 2099-2106. https://doi.org/10.1007/s11837-017-2540-2

[16] Yeh, J. W. Alloy design strategies and future trends in high-entropy alloys. JOM, 2013, 65, 1759-1771. https://doi.org/10.1007/s11837-013-0761-6

[17] Liao, Y.C.; Li, T.H.; Tsai, P.H.; Jang, J.S.C.; Hsieh, K.C.; Chen, C.Y.; Huang, J.C.; Wu, H.J.; Lo, Y.C.; Huang, C.W.; *et al*. Designing novel lightweight, high-strength and high-plasticity Tix(AlCrNb)100-x medium-entropy alloys. Intermetallics 2020, 117, 106673. https://doi.org/10.1016/j.intermet.2019.106673

[18] Chen, P.-S.; Shiu, S.-J.; Tsai, P.-H.; Liao, Y.-C.; Jang, J.S.-C.;Wu, H.-J.; Chang, S.-Y.; Chen, C.-Y.; Tsao, I.-Y. Remarkable Enhanced Mechanical Properties of TiAlCrNbV Medium-Entropy Alloy with Zr Additions. Materials, 2022, 15, 6324. https://doi.org/10.3390/ma15186324

[19] Senkov, O.N.; Semiatin, S.L. Microstructure and Properties of a Refractory High-Entropy Alloy after Cold Working. J. Alloys Compd. 2015, 649, 1110-1123. https://doi.org/10.1016/j.jallcom.2015.07.209

[20] Hou, J.; Zhang, M.; Ma, S.; Liaw, P.K.; Zhang, Y.; Qiao, J. Strengthening in Al0.25CoCrFeNi high-entropy alloys by cold rolling. Mater. Sci. Eng. 2017, 707, 593-601. https://doi.org/10.1016/j.msea.2017.09.089

[21] Eleti, R.R.; Raju, V.; Veerasham, M.; Reddy, S.R.; Bhattacharjee, P.P. Influence of strain on the formation of cold-rolling and grain growth textures of an equiatomic HfZrTiTaNb refractory high entropy alloy. Mater. Charact. 2018, 136, 286-292. https://doi.org/10.1016/j.matchar.2017.12.034

[22] Huang, Y.C.; Lai, Y.C.; Lin, Y.H.; Wu, S.K. A study on the severely cold-rolled and annealed quaternary equiatomic derivatives from quinary HfNbTaTiZr refractory high entropy alloy. J. Alloys Compd. 2021, 855, 157404. https://doi.org/10.1016/j.jallcom.2020.157404

[23] Yao, M.; Pradeep, K.; Tasan, C.; Raabe, D. A novel, single phase, non-equiatomic FeMnNiCoCr highentropy alloy with exceptional phase stability and tensile ductility. Scr. Mater. 2014, 72–73, 5-8. https://doi.org/10.1016/j.scriptamat.2013.09.030

[24] Liao, Y.C.; Chen, P.S.; Tsai, P.H.; Jang, J.S.C.; Hsieh, K.C.; Chang, H.W.; Chen, C.Y.; Huang, J.C.; Wu, H.J.; Lo, Y.C.; Huang, C.W.; Tsao, I.Y. Effect of thermomechanical treatment on the microstructure evolution and mechanical properties of lightweight Ti65(AlCrNb)35 medium-entropy alloy. Intermetallics, 2022, 143, 107470. https://doi.org/10.1016/j.intermet.2022.107470

[25] Zhang, Y.; Zhou, Y.J.; Lin, J.P.; Chen, G.L.; Liaw, P.K. Solid-solution phase formation rules for multi-component alloys. Adv. Eng. Mater. 2008, 10, 534-538. https://doi.org/10.1002/adem.200700240

[26] Liao, Y.; Ye, W.; Chen, P.; Tsai, P.; Jang, J.; Hsieh, K.; Chen, C.; Huang, J.; Wu, H.; Lo, Y.; Huang, C.; and Tsao, I.. Effect of Al concentration on the microstructural and mechanical properties of lightweight Ti60Alx(VCrNb)40-x medium-entropy alloys. Intermetallics, 2021, 135, 107213. https://doi.org/10.1016/j.intermet.2021.107213

Received on 19-01-2024 Accepted on 24-02-2024 Published on 04-03-2024

DOI: https://doi.org/10.31875/2410-4701.2024.11.01

© 2024 Chen *et al.*; Zeal Press.
This is an open access article licensed under the terms of the Creative Commons Attribution License (http://creativecommons.org/licenses/by/4.0/) which permits unrestricted use, distribution and reproduction in any medium, provided the work is properly cited.